Earth, Planets and Space

FULL PAPER Open Access

Observation of ionospheric Alfven resonator with double spectral resonance structures at low latitude station, Shillong (*dipoleL* = 1.08)

P. Adhitya[1*], Masahito Nosé[2], Jayashree Bulusu[1], Geeta Vichare[1] and A. K. Sinha[3]

Abstract:

Spectral Resonance Structures (SRS) of Ionospheric Alfven Resonator (IAR) are investigated by analysing the magnetic field data of a high sampling frequency induction coil magnetometer, installed at a low latitude Indian station, Shillong(25.56°*N*, 91.86°*E*, *dipoleL* = 1.08). One of the distinguishing features of IAR resonance structure observed at this latitude is the excitation of two spectral resonance structures simultaneously, one with a small frequency separation and the other with a large frequency separation of subsequent harmonics. The seasonal variation shows that the occurrence of double SRS is more favoured during winter, where, out of the total IAR events observed during winter, about 47% show clear signatures of double SRS and no double SRS are observed during summer. We have examined the altitudinal variation of refractive index using IRI 2016 model to understand the role of local ionospheric conditions in the formation of double spectral resonance structures. Our study reveals that the excitation of double SRS is related to the E-region to F-region variability of refractive index of the ionosphere. We also report that the double spectral resonance structures at Shillong are always observed only in the B_x component of the magnetic field variation.

Keywords: Ionospheric Alfven Resonator, Spectral Resonance Structures, Ionospheric cavity

Introduction

Ionospheric Alfven Resonator (IAR) is a feature observed in the background noise of the dynamic spectrum of geomagnetic variations in the frequency range between 0.1 and 10 Hz. The existence of IAR was first theoretically predicted by Polyakov (1976). Later the first observational evidence of IAR was given by Belyaev et al. (1990). One of the main sources of excitation of IAR is believed to be the electromagnetic emissions originating from the global thunderstorm activities (Belyaev et al. 1989a, 1989b, 1990; Nosé et al. 2017). At middle and low latitudes, lightning discharge due to local thunderstorm activity may also partly contribute to the excitation of IAR (Nosé et al. 2017; Schekotov et al. 2011; Surkov et al. 2006). IAR is formed in the ionospheric cavity bounded by the top side of the conducting E-layer as the lower boundary and the region of strong gradient in Alfven speed above the F-layer as the upper boundary. Shear Alfven waves get partially reflected along the geomagnetic field line in this cavity exciting multiple harmonics in the form of spectral resonance structures (SRS). The resonance frequencies of the SRS generally fall in the Pc1 range of ULF waves, ranging from 0.1 Hz to 10 Hz, but some studies have observed IAR events with frequencies going as high as 20–30 Hz (e.g. Beggan and Musur 2018; Simões et al. 2012). The properties of IAR depend on the mass density of ions along the magnetic field lines as well as the vertical gradient of ion density which decides the size of the ionospheric cavity. Thus, the study of IAR becomes very important as it can be used as a diagnostic tool to give an account of the local ionospheric conditions.

*Correspondence: adhitya.leo@gmail.com

[1] Indian Institute of Geomagnetism, New Panvel, Navi Mumbai, India
Full list of author information is available at the end of the article

The examination of IAR by ground observations have been carried out extensively at high and middle latitudes by various group of researchers (Beggan 2014; Beggan and Musur 2018; Belyaev et al. 1989a, 1990; Belyaev et al. 1999; Hebden et al. 2005; Molchanov et al. 2004; Parent et al. 2010; Semenova and Yahnin 2008; Surkov et al. 2006; Yahnin et al., 2003). Low latitude observations of IAR are made at Crete, Greece ($L = 1.3$) (Bösinger et al. 2002, 2004) and Muroto, Japan ($dipoleL = 1.206$) (Nosé et al. 2017). Thus, the low latitudinal extent of ground observation of IAR is only till$dipoleL = 1.206$. Simões et al. (2012) reported the electric field signatures of IAR at equatorial latitude detected by the Communications/Navigation Outage Forecasting System (C/NOFS) satellite. At high and middle latitudes, the magnetic field has a prominent component in the vertical direction which aids the formation of ionospheric cavity due to the vertical gradient of ion mass density along the field line. At low latitude the magnetic field has a more inclined component and because of such different orientation of magnetic field as compared to high and mid latitudes, certain different characteristics of IAR are observed at low latitudes. IAR has a strict night time occurrence at low latitudes (Bösinger et al. 2002; Nosé et al. 2017), whereas at high and middle latitudes IARs mostly occur during night time, but day time IARs are also observed (Yahnin et al. 2003). Also the frequency separation between the harmonics of IAR (Δf) observed at low latitudes is smaller as compared to high latitudes (Bösinger et al. 2002, 2004; Nosé et al. 2017). Bösinger et al. (2004) reported the IAR with$\Delta f \sim 0.8Hz$, in addition to the SRS with very small frequency separation, as small as$0.12Hz$, terming them as Fine Spectral Resonance Structures (FSRS). They associated the FSRS to a coupled system of ionospheric and magnetospheric Alfven resonator (IMAR), which causes the splitting of eigen frequencies.

In the present paper, we report the presence of double spectral resonance structure feature of IAR at very low subtropical latitude (dipole $L = 1.08$) Indian station, Shillong ($25.56°N, 91.86°E$). We observe very peculiar features of IAR in this region, i.e. the excitation of two spectral resonance structures simultaneously one with small Δf and other with large Δf. Although Bösinger et al. (2004) have not explicitly stated, their observations also indicated the presence of double spectral resonance structures. In the current study, the frequency separation for SRS with small Δf is approximately $0.3 - 0.4Hz$ and for large SRS $\Delta f \sim 1.3 - 1.7Hz$. We have attempted to relate the occurrence of such double spectral resonance structure to the local ionospheric conditions.

Data and observations of IAR at Shillong

An Induction coil magnetometer (ICM) LEMI-132 (procured from Lviv Center of Institute of Space Research, Ukraine) is installed at Shillong ($lat 25.56°N, long 91.86°E$), India. LT at Shillong is ($UT + 5 : 30$). The ICM consists of three induction coil magnetic sensors and communication and data acquisition system. Two of the sensors are aligned in geographic north–south direction (B_x) and east–west (B_y) in the horizontal plane and the third sensor is placed in the vertical direction (B_z). The ICM measures the magnetic field variations with a sampling frequency of 64 Hz. In the current study, the ICM data from Shillong observatory during January 2018–December 2018 are used. To construct the dynamic spectrum of B_x and B_y the magnetic variations are downsampled to 16 Hz. Hamming window is applied to a segment of 1024 data points, with 50% overlapping and then it is subjected to Fourier transform. The spectrogram of ellipticity (ϵ) is also obtained. Ellipticity is defined as $\epsilon = (L - R)/(L + R)$, where L and R are the amplitudes of left-handed and right-handed polarized waves, respectively. If X and Y be the amplitudes and θ_x and θ_y be the phase of B_x and B_y components, respectively, then L and R are computed as $L = \frac{1}{2}\sqrt{X^2 + Y^2 - 2XY\sin(\theta_x - \theta_y)}$ and $R = \frac{1}{2}\sqrt{X^2 + Y^2 + 2XY\sin(\theta_x - \theta_y)}$. The positive value of ϵ means left-hand polarization and negative values means right-hand polarization and $\epsilon = 0$ means linear polarization (Nosé et al. 2017 and references therein).

A typical example of IAR observed at Shillong is shown in Fig. 1. IARs are observed during night times. Figure 1a–b shows the dynamic power spectrum of magnetic field variations of B_x and B_y components and Fig. 1c shows the dynamic spectrum of ellipticity (ϵ), shown for 14–24 UT, as it corresponds to local night (19.5–5.5 LT). To study the characteristics of SRS, we generally look into the difference in the frequencies of the adjacent harmonics (Δf), rather than their absolute values. In all the three dynamic spectrums (Fig. 1a–c) resonance structures can be seen as rising tones starting from 14 UT, which is local evening at Shillong. It reaches its maximum around local midnight from 19 to 21 UT and then the resonance structures decay as it approaches local dawn around 24 UT.

Observation of double spectral resonance structures

December 4, 2018, event

A typical example of IAR with double spectral resonance structures is observed on December 4, 2018 (Fig. 2). In

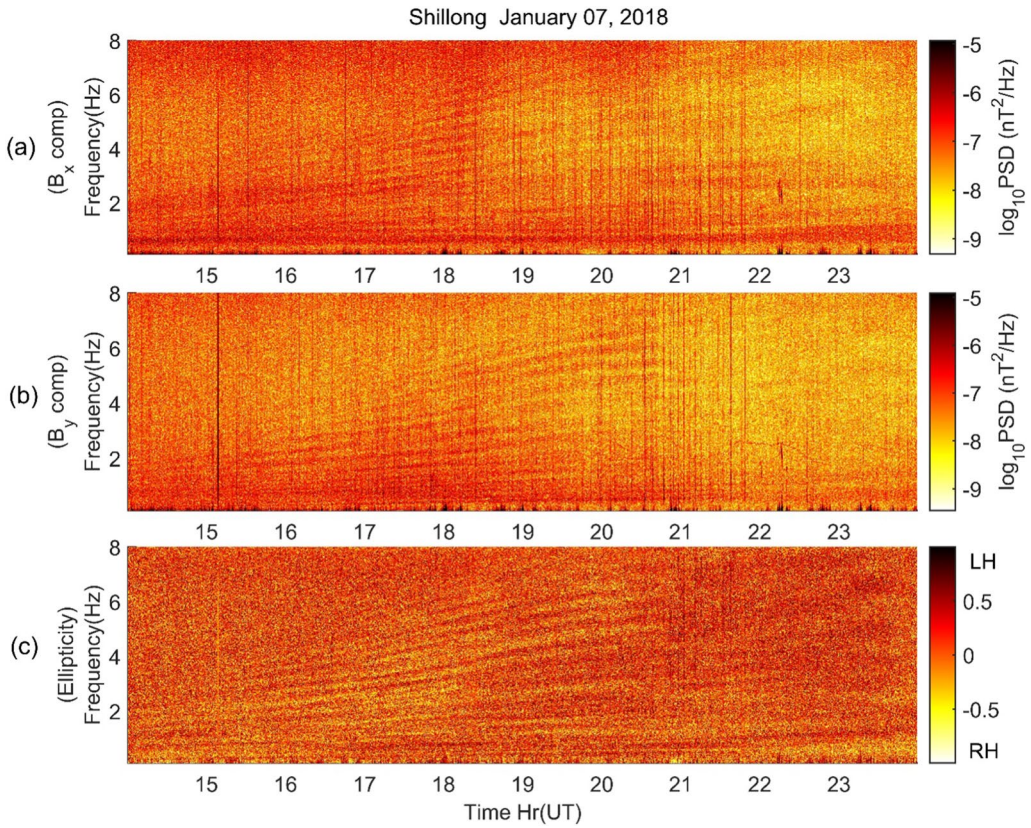

Fig. 1 Dynamic spectra of B_x (**a**), B_y (**b**) components and ellipticity (ϵ) (**c**) as an example of IAR observed at Shillong station

the dynamic power spectrum of B_x component we can observe two resonance structures being simultaneously excited. SRS with large Δf values (shown by the solid arrows) can be seen from around 14 UT, whereas the SRS with small Δf start to form prominently from around 18 UT. This can also be visualized from Fig. 3 which displays the power spectra of B_x component with the frequency resolution of 0.0156 Hz in every 1-h intervals starting from 14 to 22 UT.

This demonstration makes it easy to visualize the evolution of IAR frequencies with every hour. Solid black lines show the frequencies of SRS with small frequency separation (Δf) for 17–22 UT. It is also clear that there exists a resonance structure with large frequency separation throughout the night time. In order to visualize such broader feature more clearly we add dashed red lines that are average with the frequency width of 0.0625 Hz. In Fig. 3a to c we can see that from 14 to 17 UT, SRS with large Δf ($\sim$1.55 Hz) are dominant, even though we can see one or two harmonics of SRS with small Δf at frequency lower than 2 Hz. But from 17 UT onwards, more number of harmonics are excited for SRS with small frequency separation ($\Delta f \sim$0.35 Hz), although the large SRS are still present. The existence of double SRS can be confirmed from both the dynamic spectrograms (Fig. 2) and the 1-h power spectra of the B_x component (Fig. 3).

But if we pay attention to the dynamic spectrogram of B_y component in Fig. 2b, we observe only one spectral resonance structure with small frequency separation ($\Delta f \sim$ 0.35Hz). SRS with large Δf are not identified in the B_y component. Clear signature of SRS with small Δf is seen from around 17 UT in the B_y component, right around the time when it is observed in the B_x component. Also, in dynamic spectrum of ellipticity (ϵ) (Fig. 2c) double SRS can be seen but not as evidently as it is observed in the B_x component.

December 10, 2018, event

Another example of IAR with double SRS is observed on December 10, 2018 (Fig. 4). Again, the double SRS with large (indicated by solid arrow) and small Δf are seen in the B_x component. Here we note that the SRS with large Δf are very clear and stand out as a dominant feature right from local dusk (11 UT) to local dawn (24 UT) (Fig. 4a). SRS with small Δf get excited after 16 UT and can be seen in the dynamic spectrum till around 20 UT.

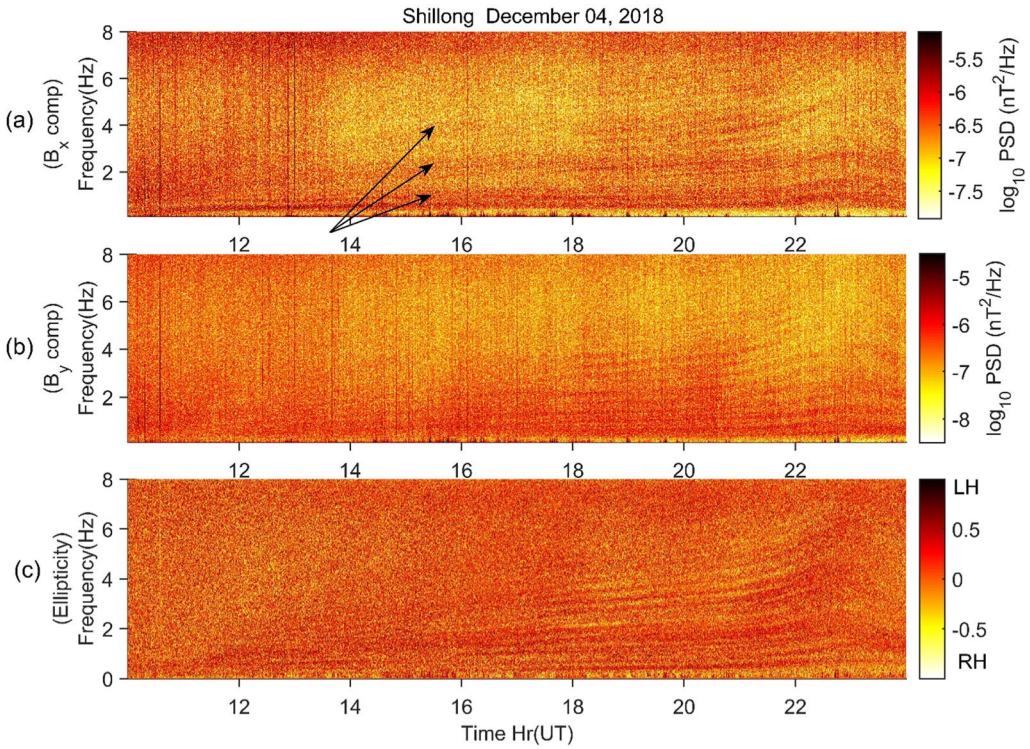

Fig. 2 Dynamic spectra of B_x (**a**), B_y (**b**) components and ellipticity (**c**), respectively, demonstrating the presence of double spectral resonance structures IAR observed at Shillong on December 04, 2018

This can also be visualized from the power spectra of the B_x component shown in Fig. 5. We can see more number of harmonics being excited with small frequency separation in Fig. 5c–f, i.e. from 16 to 20 UT.

Even though the SRS with large Δf are observed as a strong feature in the B_x component and also in the ellipticity plot, no harmonics with large Δf are present in the B_y component. (Fig. 4b). In the B_y component we can observe only one resonance structure with small Δf, around 17–21 UT.

As it is seen in the above two examples, IAR with double spectral resonance structures is clearly observed in the B_x component and not in the B_y component, for all the events observed throughout the year of 2018. Hence, the presence of double SRS can be confirmed by looking into the dynamic spectrum and power spectra of the B_x component.

Seasonal dependence of the occurrence of IAR with double spectral resonance structures IAR

We scanned for the presence of IAR with double SRS for the period of January 2018 to December 2018. Figure 6 shows the occurrence distribution of IAR with single and double SRS. IAR with double spectral resonance structures is observed only in the months of January to March and September to December with maximum occurrence during winter, while IAR with at least one SRS is observed in all months. This finding is consistent with Bösinger et al. (2004). Depending upon the survey of several cases, Bösinger et al. (2004) stated that the fine spectral resonance structures (FSRS) ($\Delta f \sim 0.12Hz$) together with SRS ($\Delta f \sim 0.8Hz$) are predominantly observed during winter. Their statistics were not good enough to present these probabilities quantitatively. In the current study it is observed that the occurrence of double SRS (SRS with small Δf and SRS with large Δf) in the months of January–April and October–December is 43% and 50%, respectively, whereas in summer, only the single SRS can be observed.

Discussion

IAR is believed to get excited in the ionospheric cavity bounded by the conducting E-layer as the lower boundary and the upper boundary forms where there is a steep gradient in the Alfven speed, $V_A = B/\sqrt{\mu_0 \rho}$, where μ_0 is permittivity of free space, B is the magnetic field, and ρ is the mass density of ions. In order to understand the cavity in which the shear Alfven waves

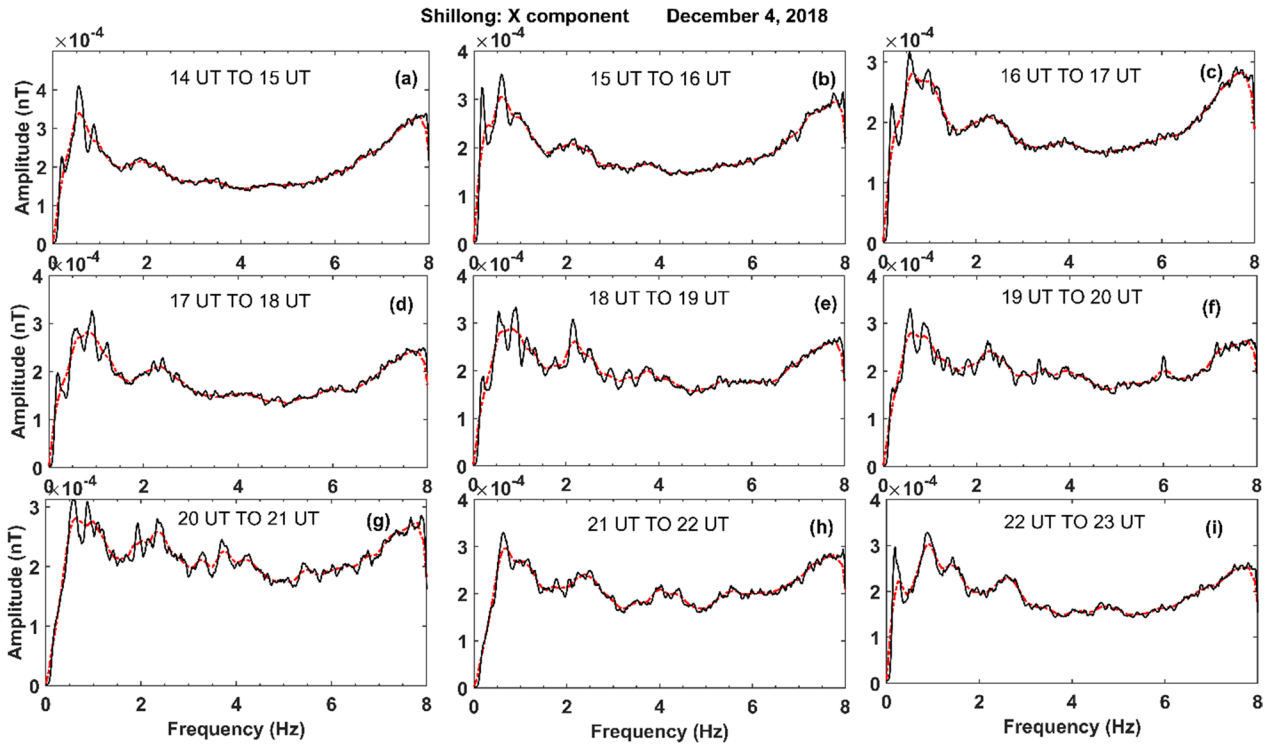

Fig. 3 Hourly static power spectra of B_x component showing the frequency separation for both small and large Spectral Resonance Structures. The solid black line is the power spectra with frequency resolution of 0.0156 Hz and dashed red line denotes the frequency resolution of 0.0625 Hz

get trapped for the excitation of IAR, the altitudinal profile of ionospheric refractive index, $n_A = c/V_A$ is obtained. Assuming charge neutrality, we use the number density of electrons and composition of ions from IRI-2016 model (Bilitza et al. 2017) to evaluate the mass density of ions (ρ). The magnitude of the magnetic field is obtained from IGRF model. Using the value of ρ and B the refractive index is calculated. Figure 7 shows the altitudinal profile of the refractive index for the hours 14UT, 17UT, 18UT, 20UT, and 23 UT of December 4, 2018 when the double SRS IAR is observed.

While examining the altitudinal profile of the refractive index, it is noticed that the depth of the well formed between the maximum refractive index ($n_{A_{max}}$) near the F-region peak (marked by red asterisks) and local minimum refractive index ($n_{A_{min}}$) in the valley region above the E-region, i.e. $d(= n_{A_{max}} - n_{A_{min}})$ becomes smaller during the period when double spectral resonance structures are excited. To verify this, the altitudinal profile of refractive index is obtained for the entire year of 2018 for the time 17 UT, 18 UT, 19 UT, and 20 UT. The depth (d) is obtained from the refractive index profile and is plotted in Fig. 8. We note that during winter, when double SRS are observed, the value of d is smaller as compared to the months of summer when only single SRS are observed. Hence, it is safe to consider that smaller value of d favours the excitation of IAR with double spectral resonance structures.

One of the characteristic features of IAR is the frequency separation (Δf) between the harmonics of its spectral resonance structures. In a previous study, Polyakov and Rapoport (1981) derived a basic and simple analytical model to calculate the separation between the resonance frequencies of IAR (Δf).

$$\Delta f_{PR} = \frac{c}{2((h_2 - h_1) + L_{sh}) n_{A_{max}}}, \tag{1}$$

where h_1 is the height of the lower boundary of the ionospheric cavity, h_2 is the height at which the refractive index starts to exponentially decrease, $n_{A_{max}}$ is the maximum refractive index, and L_{sh} is the scale height of the exponential decrease of refractive index above $n_{A_{max}}$ at the F-region peak. All the parameters for the calculation of Δf are obtained from the vertical profile of the refractive index (Fig. 7), using the same method used by Nosé et al. (2017). A simple analytical n_A model expressed as a function of altitude given by Polyakov and Rapoport (1981) is used.

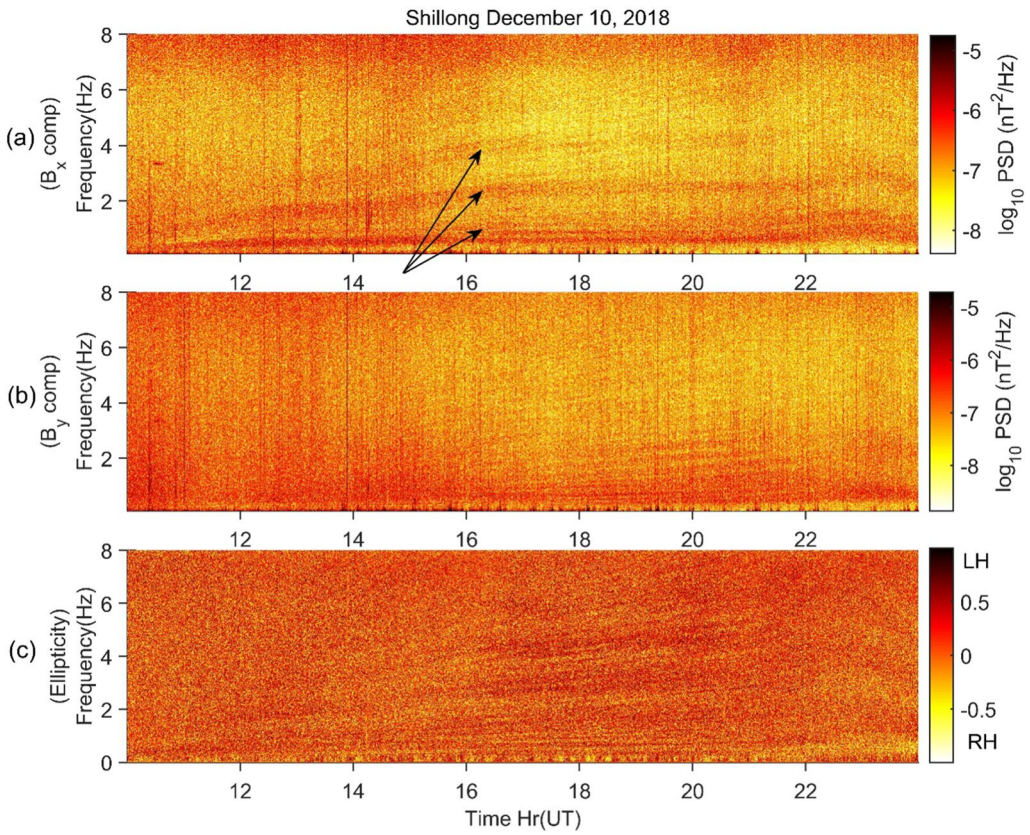

Fig. 4 Dynamic spectra of B_x (**a**), B_y (**b**) components and ellipticity (**c**), respectively, demonstrating the presence of double spectral resonance structures IAR observed at Shillong on December 10, 2018

$$n_A^2(z) = n_{A_{max}}^2 \left\{ \delta^2 + \exp\left(-\left(\frac{2(z-h_2)}{L_{sh}} \right) \right) \right\} (z > h_2).$$
$$n_A^2(z) = n_{A_{max}}^2 (h_1 < z < h_2) \tag{2}$$

The analytical n_A models are fit to the altitude profiles given in Fig. 7. The value of $n_{A_{max}}$ is set to the maximum value of the n_A profile and h_1 is taken to be the height where n_A has a local minimum between the E- and F-layers, $\delta = n_0/n_{A_{max}}$, where n_0 is the value of n_A at $z = 2000km$. Then, Eq. (2) is computed for various integer values of h_2 and L_{sh} and we look for the values of h_2 and L_{sh} that minimize the difference in n_A between the analytical model and the altitude profile in Fig. 7. The frequency separation, Δf, is calculated for the IAR event observed on December 4, 2018. As explained in "December 4, 2018, event" Section, we observe double spectral resonance structure on December 4, 2018, i.e. two SRS with different Δf are excited simultaneously. Hence, we have two observed values of Δf values for the given event.

In Table 1, the second and third columns show the observed value of frequency separation Δf, and the fourth column shows the frequency separation values calculated using Polyakov and Rapoport (1981) model (Δf_{PR}). SRS with large Δf can be observed from 14 UT, but SRS with small Δf are clearly observed from 16UT – 20 UT. It is clearly seen that Δf_{PR} does not match well with the observed value of Δf. This could be because Polyakov and Rapoport (1981) model considers the field lines to be vertical. But at low latitudes the field lines are inclined. One of the effects of inclination is the change in the height of the ionospheric cavity. We tried to modify Eq. (1) by including the effect of inclination angle on the height of the cavity. The equation is modified as

$$\Delta f_{PR_{mod}} = \frac{c}{2\left(\frac{(h_2-h_1)}{\sin\alpha} + \frac{L_{sh}}{\sin\alpha} \right) n_{A_{max}}}, \tag{3}$$

where α is the inclination angle. Fifth column of Table 1 shows the frequency separation ($\Delta f_{PR_{mod}}$) of the resonance structures calculated by using Eq. (3). We see some improvement in $\Delta f_{PR_{mod}}$ as compared to Δf_{PR}, but still it does not match very well with the observed Δf. A simple adjustment to height of the ionospheric cavity by taking into account the magnetic inclination may

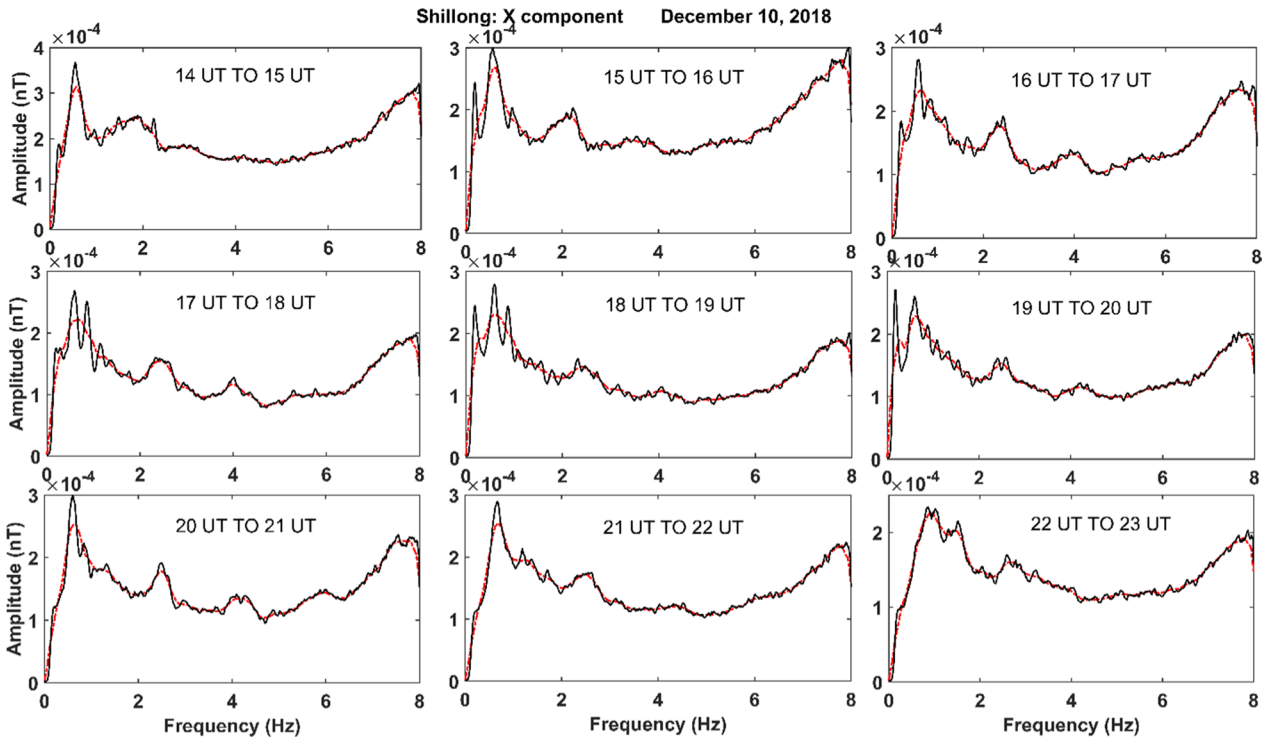

Fig. 5 Hourly static power spectra of B_x component showing the frequency separation for both small and large Spectral Resonance Structures. The solid black line is the power spectra with frequency resolution of 0.0156 Hz and dashed red line denotes the frequency resolution of 0.0625 Hz

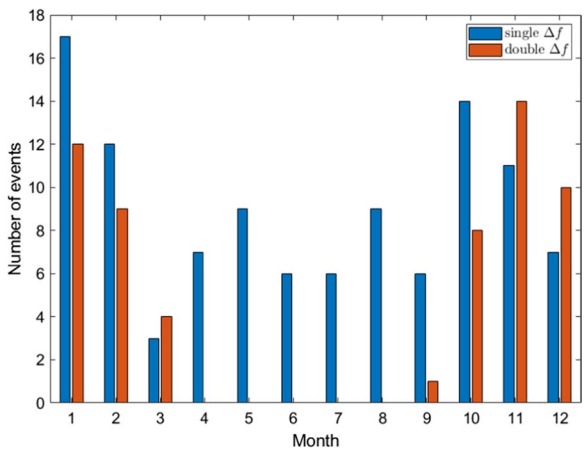

Fig. 6 Seasonal variation of occurrence of IAR with single as well as double Spectral Resonance Structures for the year 2018

not be enough at low latitudes. Therefore, the simple analytic model of Polyakov and Rapoport (1981) may not give the exact estimations at low latitudes, but still it can be used to obtain the rough estimate of Δf for SRS within the ionospheric cavity. The effect of magnetic inclination on IAR is explained in detail by Bösinger et al. (2009). Moreover, if the field lines are completely immersed in the ionospheric cavity then the model may not be appropriate. However, at the station of present study, with $L = 1.08$, the maximum height of the field line is $h \cong (L-1)R_0 \cong 510km$, where R_0 is the radius of Earth, which is generally above the upper boundary of ionospheric cavity, and hence, the model can be used for approximate estimations. Even though the analytically obtained frequency separation ($\Delta f_{PR_{mod}}$) does not give the correct estimation at low latitudes, still it is closer to the observed Δf for large SRS. Hence, we can say that the SRS with large Δf may have formed within the ionospheric cavity bounded by the region above conducting E-region and the top side of the F-layer peak.

As for the SRS with small Δf, the shear Alfven waves should have been reflected from a larger cavity. One such case could be the Field Line Resonance (FLR), where the Alfven waves are reflected from the conjugate points of the field line. At very low latitude like Shillong, the total length of the field line between the conjugate ground points is $l = R_0 L \int_{-\lambda_c}^{\lambda_c} \cos\lambda \sqrt{1+3\sin^2\lambda} d\lambda \cong 0.56 R_0 L \cong 3854km$, where λ is the magnetic latitude along and λ_c is the magnetic latitude at the conjugate point. The harmonic frequencies of the Alfven waves reflected from the

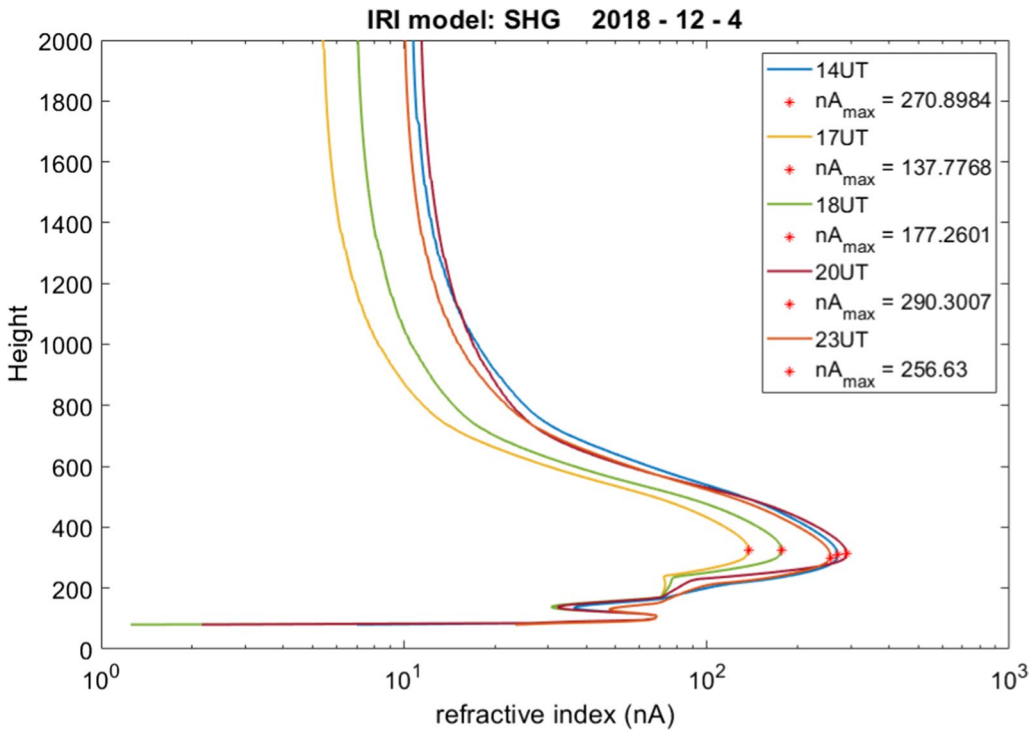

Fig. 7 Altitudinal profile of refractive index obtained by using IRI 2016 model for various UT on December 04, 2018

conjugate points of such field lines are in the same range as the spectral resonance structures excited within the ionospheric cavity. This finding is again consistent with Bösinger et al. (2004). The frequency separation of FSRS observed by Bösinger et al. (2004) was $\Delta f \sim 0.12Hz$, while in our study the frequency separation of SRS with small Δf is $\sim 0.3 - 0.4Hz$. This difference in Δf between the two observations could be because of the different latitudes at which the observations are made. Bösinger et al. (2004) observed fine spectral resonance structure (FSRS) at Crete ($L = 1.3$) where the length of the field line is longer than the length of the field line at Shillong ($dipoleL = 1.08$). SRS due to reflection from the conjugate points of longer field line will have a smaller frequency separation (Δf). Hence, by looking into the observations of previous and current studies, it is very likely that the SRS with small Δf could be a result of reflection of Alfven waves from the conjugate points of the field lines. It can be summarized that the SRS with large $\Delta f (\sim 1.3 - 1.7Hz)$ excited within the ionospheric cavity together with SRS with small $\Delta f (\sim 0.3 - 0.4Hz)$ excited between the conjugate points of the field line give rise to the double spectral resonance structures observed at the ground station, Shillong. A pictorial representation of excitation of double SRS due to ionospheric cavity and field line oscillations is shown in Fig. 9.

At very low latitudes, where the length of the field line becomes comparable to the ionospheric height, the SRS observed at ground are affected by both Ionospheric Alfven Resonator and Magnetospheric field line Resonator (Bösinger et al. 2004; Fedorov et al. 2016). We calculate the frequency separation (Δf) for ionospheric cavity during summer when d is large, which falls in the range$\sim 0.4 - 0.6Hz$. These Δf values are similar to the Δf of SRS observed due to magnetospheric cavity during winter which is in the range $\sim 0.3 - 0.4Hz$ (Table 1). Since the length of the field line as well as the density distribution of plasma along the field line does not vary much with season, it can be assumed that the frequency separation Δf of SRS due to magnetospheric cavity does not change much in summer. Therefore, it can be considered that the SRS due to ionospheric cavity and magnetospheric cavity become very similar and appear as a single SRS during summer. In this situation, it becomes difficult to distinguish between the cavities (ionospheric or magnetospheric) within which the SRS are formed. On the other hand, during winter when d is small, the frequency separation (Δf) of SRS due to ionospheric cavity increases ($\Delta f \sim 1.3 - 1.7Hz$) and becomes distinguishingly different than the Δf due to magnetospheric cavity($\Delta f \sim 0.3 - 0.4Hz$). As a result we can observe two distinct SRS. Thus, the depth of the cavity (d) can be used

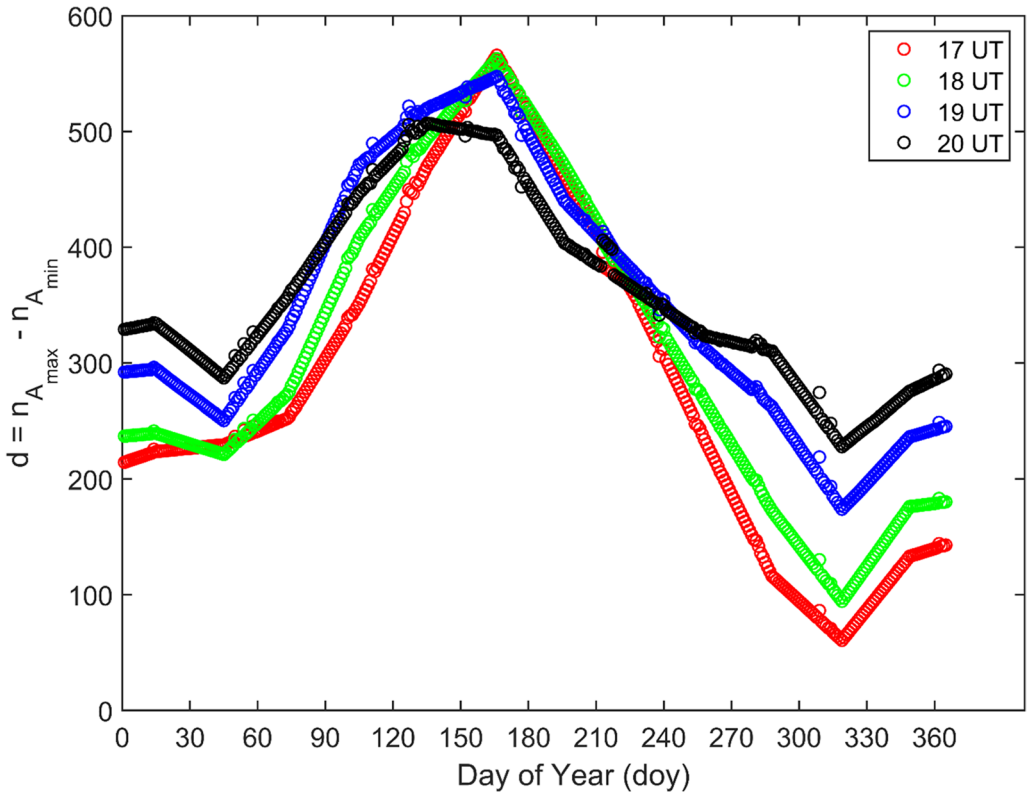

Fig. 8 The value of depth of the well formed by the minimum and maximum refractive index at the region above the E-layer and the F-layer peak, respectively, $d = (n_{A_{max}} - n_{A_{min}})$ plotted for the entire year of 2018

Table 1 Comparison between the frequencies separation obtained from observations of double spectral resonance structures observed on December 4, 2018 and from analytical model

UT	Observed Δf (Hz)		Analytical Δf_{PR} (Hz) Polyakov and Rapoport [1981]	Analytical Δf_{PRmod} (Hz) Modified by including inclination angle
	Small Δf	Large Δf		
15	–	1.5	1.8424	1.1708
16	0.4062	1.625	2.5111	1.5957
17	0.3125	1.5	2.7355	1.7378
18	0.3594	1.375	2.1478	1.3642
19	0.2960	1.6875	1.5664	0.9953
20	0.3125	1.6875	1.3181	0.8377
21	–	1.6875	1.3781	1.0276

as a proxy for observing double spectral resonance structures. Smaller the value of$d$, higher is the probability of observing double SRS.

In "Observation of double spectral resonance structures" Section, it has been discussed that double spectral resonance structures are observed in the B_x component, whereas in the B_y component we observe only the SRS with small Δf, which are associated with a larger cavity. During winter, when double SRS are excited, the B_y component does not detect the signatures of SRS which are formed due to the ionospheric cavity. This could also be visualized in Fig. 10, which is the power spectra of B_x and B_y component as observed on December 4, 2018, when double SRS are observed. The broader features like the SRS with large $\Delta f (\sim 1.4 Hz)$ are seen along with SRS with small $\Delta f (\sim 0.35 Hz)$ in the X component, whereas in the Y component only one spectral resonance structure is seen with $\Delta f \sim 0.35 Hz$. Belyaev et al. (1989b) developed a theory that suggested that the resonant structures are observed in one of the two orthogonal components, that is along the direction of the source. In our observations we see that SRS due to ionospheric cavity is always observed in the B_x component only, throughout the winter. In view of the theory of Belyaev et al. (1989b), does our observations suggest that the source responsible for the excitation of SRS within ionospheric cavity during winter is always the same, and in the same direction? Also Bösinger et al. (2009) suggested that the inclination

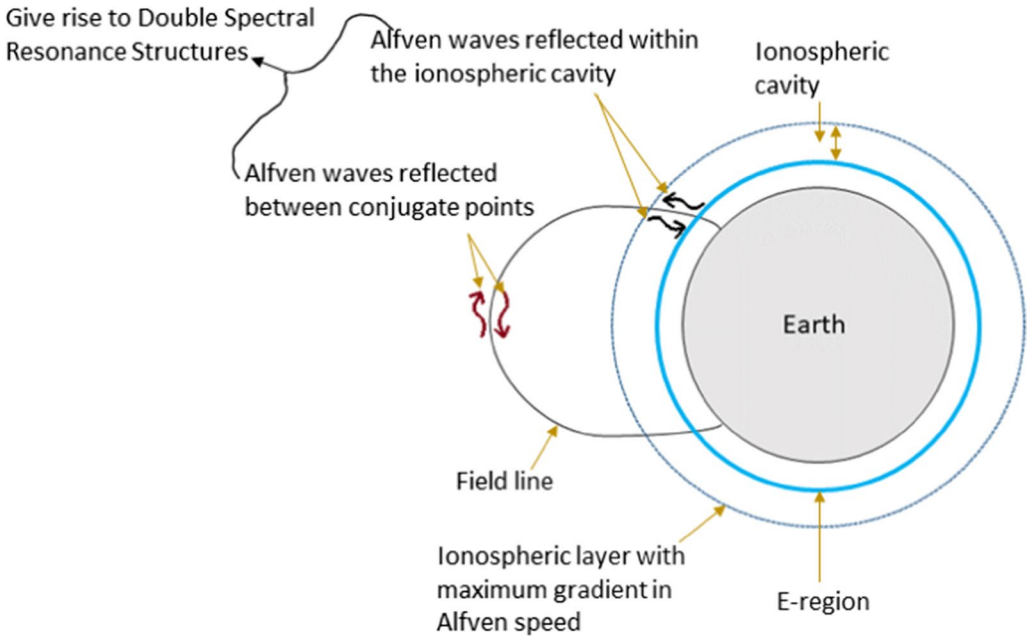

Fig. 9 Pictorial representation of a possible mechanism of excitation of double spectral resonance structures

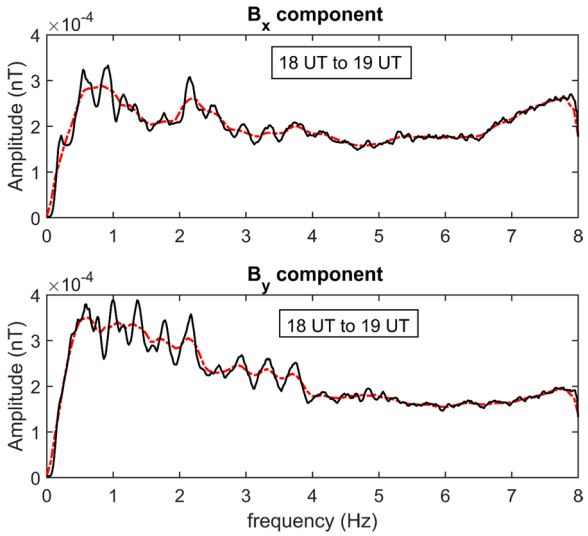

Fig. 10 Power spectra of B_x and B_y component observed on December 4, 2018. The solid black line is the power spectra with frequency resolution of 0.0156 Hz and dashed red line denotes the frequency resolution of 0.0625 Hz

of the magnetic field lines at low latitudes lead to the dependence of field components on the wave angle ϕ which is defined as the angle between the direction of the source and the normal to the magnetic meridian passing through the observation site. This may consequently result in the observation of SRS of Ionospheric Alfven Resonator in both the orthogonal components. But again, this is in contrast with our observations. In fact, we speculate that this could be because of the condition of the ionospheric cavity during winter. During winter $d(= n_{A_{max}} - n_{A_{min}})$ is small (Fig. 8) which means a smaller gradient of refractive index within the ionospheric cavity. This may result in less reflection of Alfven waves within the ionospheric cavity and may lead to the observation of IAR only in one prominent direction. The study of the sources responsible for the excitation of SRS within the ionospheric Alfven resonator could shed some light on the observation of SRS due to ionospheric cavity preferred in the B_x component. The absence of clear signatures of SRS due to ionospheric cavity in the B_y component during winter have raised a few questions which we are unable to decipher in the current study. In this regard a detailed investigation is required and will form a part of our future study.

Summary and conclusion

We analysed the magnetic variation data from Induction Coil Magnetometer installed at a low latitude station, Shillong for a duration of January–December, 2018. We observed a distinct feature of double spectral resonance structures (SRS) being excited. In the previous studies, there was only one indication of such an observation of double SRS at low latitude by Bösinger et al. (2004) at Crete ($L = 1.13$). The current work presents a more systematic study of double SRS at a lower

latitude ($dipoleL = 1.08$). The one year statistical study reveals that during summer we observe excitation of strictly one SRS and during winter two SRS are simultaneously excited. By computing the frequency separation (Δf) between the subsequent resonant harmonics using Polyakov and Rapoport (1981) model, it is seen that the SRS with large $\Delta f (\sim 1.3 - 1.7 Hz)$ are the result of IAR within the ionospheric cavity. The SRS with small $\Delta f (\sim 0.3 - 0.5 Hz)$ may be excited within a larger cavity, such as reflection of Alfven waves between conjugate points along the field line.

We studied the ionospheric conditions for the formation of IAR by obtaining the altitudinal profile of the refractive index using IRI 2016 model. The depth of the well of the refractive index (d), formed by the local minimum of the refractive index in the valley region above the E-region and the maximum refractive index at the F-region peak, is estimated for the entire year of 2018. It is observed that during winter d decreases, which favours the excitation of double SRS. Smaller d results in ineffective trapping of Alfven waves within the ionospheric cavity, and the Alfven waves are also reflected from a larger cavity, resulting in the observation of double SRS. Hence, during winter the trapping of Alfven waves in a larger cavity, like between the conjugate points of a field line, gives rise to SRS with small frequency separation and Alfven waves trapped within the ionospheric cavity gives rise to SRS with large frequency separation.

It is also noticed that whenever double spectral resonance structures are excited, the SRS due to the larger cavity are observed in both B_x and B_y components, but SRS due to the ionospheric cavity are observed only in the B_x component. We contemplate that this behaviour may be due to the smaller gradient of refractive index within the ionospheric cavity as well as the direction of the source exciting the IAR during winter. To get a clear and complete picture of this phenomenon more analyses have to be performed and a detailed study of the sources responsible for the excitation of IAR and the role of ionospheric conditions related to IAR has to be carried out in future.

Abbreviations

SRS: Spectral Resonance Structures; IAR: Ionospheric Alfven Resonator; ULF: Ultra-Low Frequency; ICM: Induction Coil Magnetometer; FSRS: Fine Spectral Resonance Structures; IMAR: Ionospheric and Magnetospheric Alfven resonator; FLR: Field Line Resonance; C/NOFS: Communications/Navigation Outage Forecasting System.

Acknowledgements

PA would like to thank Prof. Shiokawa for the support under JSPS Core-to-Core program.

Author contributions

MN, JB, and PA were involved in conceptualizing the idea. PA has carried out the data analysis and prepared the manuscript. MN, JB, GV, and AKS contributed in the discussion and interpretations of the results. The manuscript was edited and revised by all the authors. All authors read and approved the final manuscript

Funding

PA is supported for this study by the Japan Society for the Promotion of Science (JSPS), Core-to-Core Program, Asia-Africa Science Platforms (Grant JPJSCCB20210003), and Grant-in-Aid for Scientific Research (B; Grant 21H01147). This work is also supported by Department of Science and Technology, Govt. of India.

Data availability

The ICM data are provided by Indian Institute of Geomagnetism and will be made available on request to Director, IIG. The ionospheric parameters obtained from IRI 2016 model is available at https://ccmc.gsfc.nasa.gov/modelweb/models/iri2016_vitmo.php. The MATLAB code for IRI 2016 model is given by Drew Compston, https://in.mathworks.com/matlabcentral/fileexchange/34863-international-reference-ionosphere-iri-model. Geomagnetic field data from the IGRF model can be obtained at https://omniweb.gsfc.nasa.gov/vitmo/cgm.html.

Declarations

Ethics approval and consent to participate

Not applicable.

Consent for publication

Not applicable.

Competing interests

The authors have no competing interests to declare.

Author details

[1]Indian Institute of Geomagnetism, New Panvel, Navi Mumbai, India. [2]Institute for Space-Earth Environmental Research, Nagoya University, Nagoya, Japan. [3]School of Science, Department of Physics, University of Bahrain, Sakhir, Bahrain.

Received: 30 June 2022 Accepted: 27 October 2022
Published online: 12 November 2022

References

Beggan CD (2014) Automatic detection of ionospheric Alfvén resonances using signal and image processing techniques. Ann Geophys 32(8):951–958. https://doi.org/10.5194/angeo-32-951-2014

Beggan CD, Musur M (2018) Observation of ionospheric Alfvén resonances at 1–30 Hz and their superposition with the Schumann Resonances. J Geophys Res Space Physics 123(5):4202–4214. https://doi.org/10.1029/2018JA025264

Belyaev PP, Polyakov CV, Rapoport VO, Trakhtengerts VY (1989a) Experimental studies of the spectral resonance structure of the atmospheric electromagnetic noise background within the range of short-period geomagnetic pulsations. Radiophys Quantum Electron 32(6):491–501. https://doi.org/10.1007/BF01058169

Belyaev PP, Polyakov SV, Rapoport VO, Trakhtengerts VY (1989b) Theory for the formation of resonance structure in the spectrum of atmospheric electromagnetic background noise in the range of short-period geomagnetic pulsations. Radiophys Quantum Electron 32(7):594–601. https://doi.org/10.1007/BF01058124

Belyaev PP, Polyakov SV, Rapoport VO, Trakhtengerts VY (1990) The ionospheric Alfven resonator. J Atmos Terr Phys 52(9):781–788. https://doi.org/10.1016/0021-9169(90)90010-K

Belyaev PP, Bösinger T, Isaev SV, Kangas J (1999) First evidence at high latitudes for the ionospheric Alfven resonator. J Geophys Res. https://doi.org/10.1029/1998JA900062

Bilitza D, Altadill D, Truhlik V, Shubin V, Galkin I, Reinisch B, Huang X (2017) International Reference Ionosphere 2016: from ionospheric climate to real-time weather predictions. Space Weather 15(2):418–429. https://doi.org/10.1002/2016SW001593

Bösinger T, Haldoupis C, Belyaev PP, Yakunin MN, Semenova NV, Demekhov AG, Angelopoulos V (2002) Spectral properties of the ionospheric Alfvén resonator observed at a low-latitude station (L = 1.3). J Geophys Res: Space Physics 107(A10):1–9. https://doi.org/10.1029/2001JA005076
Bösinger T, Demekhov AG, Trakhtengerts VY (2004) Fine structure in ionospheric Alfvén resonator spectra observed at low latitude (L = 1.3). Geophys Res Lett 31(18):1–5. https://doi.org/10.1029/2004GL020777
Bösinger T, Ermakova EN, Haldoupis C, Kotik DS (2009) Magnetic-inclination effects in the spectral resonance structure of the ionospheric Alfvén resonator. Ann Geophys 27(3):1313–1320. https://doi.org/10.5194/angeo-27-1313-2009
Fedorov E, Mazur N, Pilipenko V, Engebretson M (2016) Interaction of magnetospheric Alfvén waves with the ionosphere in the Pc1. J Geophys Res. https://doi.org/10.1002/2015JA021020
Hebden SR, Robinson TR, Wright DM, Yeoman T, Raita T, Bösinger T (2005) A quantitative analysis of the diurnal evolution of Ionospheric Alfvén resonator magnetic resonance features and calculation of changing IAR parameters. Ann Geophys 23(5):1711–1721. https://doi.org/10.5194/ANGEO-23-1711-2005
Molchanov OA, Schekotov AY, Fedorov E, Hayakawa M (2004) Ionospheric Alfven resonance at middle latitudes: results of observations at Kamchatka. Phys Chemis Earth, Parts a/b/c 29(4–9):649–655. https://doi.org/10.1016/J.PCE.2003.09.022
Nosé M, Uyeshima M, Kawai J, Hase H (2017) Ionospheric Alfvén resonator observed at low-latitude ground station, Muroto. J Geophys Res Space Physics 122(7):7240–7255. https://doi.org/10.1002/2017JA024204
Pasrent A, Mann IR, Rae IJ (2010) Effects of substorm dynamics on magnetic signatures of the ionospheric Alfvén resonator. J Geophys Res: Space Physics. https://doi.org/10.1029/2009JA014673
Polyakov SV (1976) On properties of an ionospheric Alfve´n resonator. In Symposium KAPG on Solar-Terrestrial Physics, Nauka, Moscow 3:72–73
Polyakov SV, Rapoport VO (1981) The ionospheric Alfvén resonator. Geomagn Aeron 21:610–614
Schekotov A, Pilipenko V, Shiokawa K, Fedorov E (2011) ULF impulsive magnetic response at mid-latitudes to lightning activity. Earth, Planets and Space 63(2):119–128. https://doi.org/10.5047/eps.2010.12.009
Semenova NV, Yahnin AG (2008) Diurnal behaviour of the ionospheric Alfvén resonator signatures as observed at high latitude observatory Barentsburg (L=15). Ann Geophys 26(8):2245–2251. https://doi.org/10.5194/angeo-26-2245-2008
Simões F, Klenzing J, Ivanov S, Pfaff R, Freudenreich H, Bilitza D, Rowland D, Bromund K, Liebrecht MC, Martin S, Schuck P, Uribe P, Yokoyama T (2012) Detection of ionospheric Alfvén resonator signatures in the equatorial ionosphere. J Geophys Res: Space Physics 1:1
Surkov VV, Hayakawa M, Schekotov AY, Fedorov EN, Molchanov OA (2006) Ionospheric Alfvén resonator excitation due to nearby thunderstorms. J Geophys Res Space Physics 111(1):1–13. https://doi.org/10.1029/2005JA011320
Yahnin AG, Semenova NV, Ostapenko AA, Kangas J, Manninen J, Turunen T (2003) Morphology of the spectral resonance structure of the electromagnetic background noise in the range of 0.1–4 Hz at L = 5.2. Annales Geophysicae 21(3):779–786. https://doi.org/10.5194/ANGEO-21-779-2003

Publisher's Note